TURBULENCE CLOSE TO A ROUGH URBAN SURFACE PART I: REYNOLDS STRESS

M. W. ROTACH

Swiss Federal Institute of Technology, Climatology Section, Dept. of Geography, Winterthurerstr. 190, CH-8057 Zürich, Switzerland

(Received in final form 28 July, 1992)

Abstract. The Reynolds stress field of the urban roughness sublayer is studied experimentally at a site in the centre of Zürich (Switzerland). Turbulence observations at various heights within and above a street canyon are used together with profiles of mean variables to determine an average profile of Reynolds stress for the lowest few tens of meters of an urban roughness sublayer.

The spatially averaged net vertical transport of momentum or Reynolds stress is found to be essentially zero at a height close to the average zero plane displacement and increases higher up in the urban roughness sublayer. A parameterisation for the height dependence is provided based on the height above zero plane displacement and a reference friction velocity. Results of a quadrant analysis for Reynolds stress indicate that eddies of the organized shear flow are broken up in the vicinity of the zero plane displacement into smaller, less correlated (random) flow patterns. Although not constant with height, turbulent flux of momentum is shown to be the relevant process for the description of the profile of mean wind speed even in the urban roughness sublayer.

1. Introduction

An urban surface consists of low and high buildings, trees and other roughness elements, which are arrayed in blocks or standing by themselves, intersected by streets, crossings or open surfaces. This complex morphology results in a modified flow and turbulence structure in the lowest few tens of meters of the urban atmosphere in contrast to the flow over 'ideal and homogeneous' surfaces. In addition, and at a larger scale, an urban boundary layer develops due to the altered roughness and thermal properties of a city as a whole. In this paper, the turbulent transport of momentum, i.e., the Reynolds stress field in the vicinity of roof level is discussed.

The lowest part of the urban boundary layer, the urban surface layer (or inner layer) has to be considered in two parts: (1) Since the ratio between the height of the boundary layer, z_i, and the height scale of the roughness elements, h, remains finite (z_i/h being of the order of 10^2) a flow region with measurable and considerable vertical extension can be found close to the surface where no inertial sublayer behaviour can be expected. Following Raupach (1981) this layer, where the turbulence structure is fully three-dimensional and depends explicitly on the properties of the roughness, will be called the roughness sublayer (RS); (2) The remaining part of the surface layer is the inertial sublayer (IS). Here, Monin–Obukhov similarity theory applies. However, it has to be noted that the roughness sublayer may, at least for certain flow conditions, extend to considerable heights,

Boundary-Layer Meteorology **65**: 1–28, 1993.

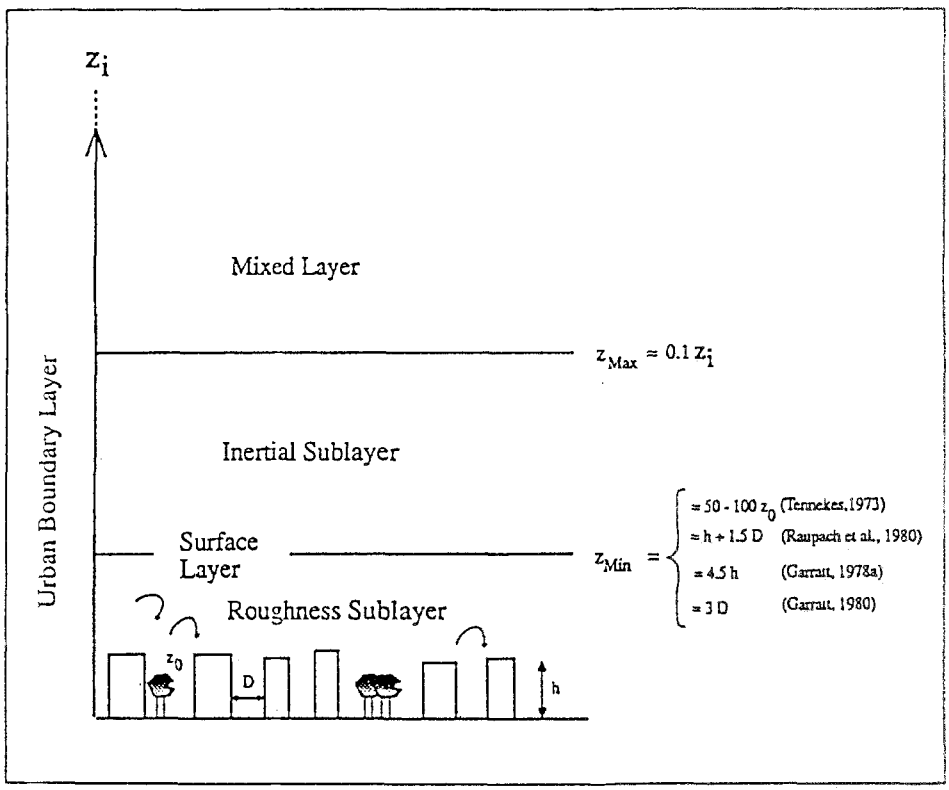

Fig. 1. Boundary-layer structure over a rough (urban) surface. A daytime situation is displayed where z_i denotes the mixed layer height. Modified after Oke (1988).

so that the inertial sublayer may be 'squeezed' between the RS and the overlying layer. This vertical structure is sketched in Figure 1. The lower boundary of the urban RS can alternatively be defined as the top of the urban canopy layer (UCL), which corresponds roughly to the average height of buildings (Oke, 1988), or as the level $z = d$, where d is the zero plane displacement. Some evidence for the latter choice will be presented in the following.

Very little is known about the characteristics of turbulence in the UCL and the urban RS. Thus urban diffusion modelling (on a local scale) is often based on Monin–Obukhov similarity theory (e.g., Gryning and Lyck, 1984; Gross, 1989), which is neither obvious nor verified. An urban environment has a great density of pollutant sources, most of them being located within the RS or the UCL, where a substantial part of the diffusion process takes place.

The measurements presented here were obtained as a part of the Zürich Urban Climate Programme between March 1987 and May 1988. In a companion paper (Rotach, 1993a, hereafter referred to as II) other findings of this study that are essential for the results on Reynolds stress are presented. In particular, it is

shown that local scaling as proposed by Högström *et al.* (1982) provides a good representation of the data within the RS. This means that, e.g., the non-dimensionalized gradient of wind speed can be described with the same semi-empirical function as in the inertial sublayer, provided that all variables are considered as local values (see also Rotach, 1990). Thus knowledge of turbulent transport of momentum (or the local friction velocity) can substantially improve the predictability of other turbulence variables (see II) and average flow properties (Section 5).

2. Measurements

Observations were taken in the city of Zürich (Switzerland) on two towers, one of them located on top of a five-story building and the other within the neighbouring street canyon. Instruments were mounted at four levels on each tower with the lowest level of the 'roof-top tower' corresponding to the highest level of the 'canyon tower' (Figure 2). The site is located in the center of the flat part of the urban area with no distinct terrain elevation within a radius of about 2 km. This part of the city is a mixed residential/commercial area that can be considered typical for a large part of the city (there is no distinct 'city center', i.e., an area with much higher buildings than the surrounding urban/suburban structure). Blocks of buildings, a few small parks and a school yard, streets and squares can be found in the close vicinity. Buildings are fairly regularly distributed within a radius of about 300 m and do not vary significantly in height (approximately 20 m). Street canyons are characterized by a height-to-width ratio of about unity.

Routine observations provided three profiles of mean wind speed, temperature and specific humidity: one on the roof-top tower (labelled 'R' in Figure 2, together with the respective height above street level), one in the middle of the street canyon (labelled 'CC', canyon centre) and one within the street canyon, closer to the wall (labelled 'CW', canyon wall). Turbulence measurements were performed with two ultra sonic anemometers in different height combinations (Table I). One instrument used was a Kaijo Denki three-dimensional probe (TR-61C) while the other combined two two-dimensional probes (Kaijo Denki TJ-51) to form a three-dimensional sensor. Both instruments were extensively tested and calibrated in a wind tunnel. The accuracy of mean values was found to be better than 4% for levelled instruments after applying a calibration scheme to individual wind vectors, mainly dependent on the direction of the approaching flow with respect to the instrument (Rotach, 1991). The uncertainty of the turbulence statistics was assessed following Wyngaard (1973):

$$a^2_{\overline{u'w'},\overline{v'w'}} = \frac{z'}{T_a \bar{u}} \left(\frac{\overline{(u'w')^2}}{u_*^4} - 1 \right), \tag{1}$$

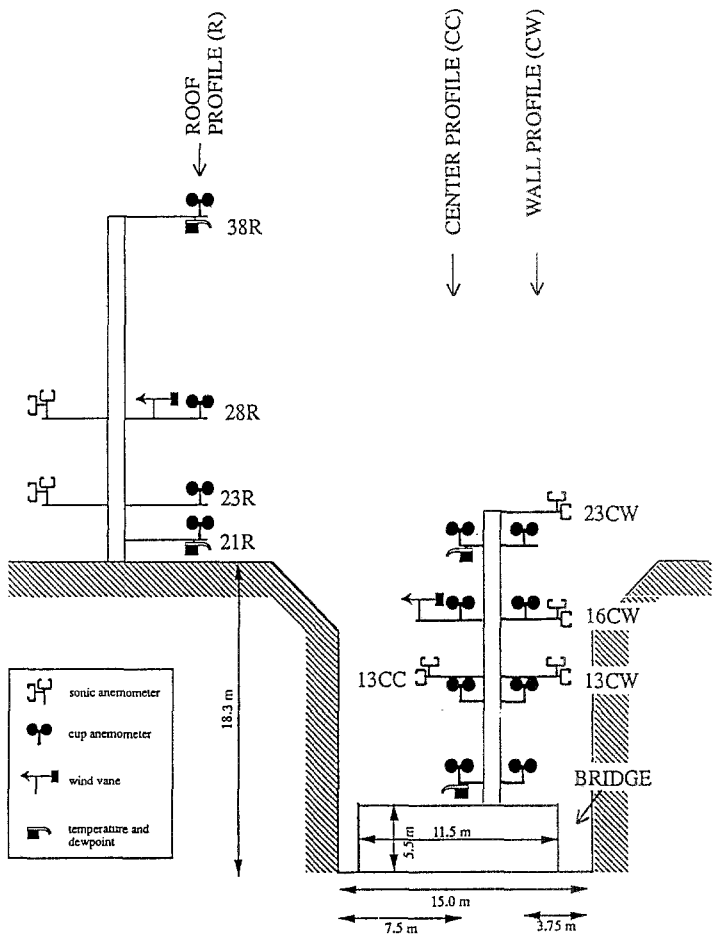

Fig. 2. Schematic view of the measurement site. The symbol for sonic anemometer denotes all (but not simultaneously) realized positions of measurements.

$$a^2_{\overline{w'\theta'}} = \frac{z'}{T_a \bar{u}} \left(\frac{\overline{(w'\theta')^2}}{u_*^2 \theta_*^2} - 1 \right), \tag{2}$$

where 'a' denotes the accuracy of the respective turbulent flux ($\overline{u'w'}$, $\overline{v'w'}$ or $\overline{w'\theta'}$), T_a is the averaging period (50 min), u_* and θ_* the friction velocity and characteristic temperature, respectively, and z' the height above zero plane displacement. If the errors for all three turbulent fluxes were smaller than 25%, a run was accepted for further analysis. The sampling frequency was $1\,s^{-1}$ for both instruments. Before the analysis was performed, all variables of each run were linearly detrended and checked for stationarity using a run test (Bendat and Piersol, 1986).

The zero plane displacement d was determined for eight separate 45°-sectors of

TABLE I

Configuration and duration of turbulence observations at the measurement site

No	3D Sonic		2 × 2D Sonic		Number of 50-min runs**		Date
	Position*	Height above street	Position*	Height above street	3D	2D	
1	23R	23.3	23R	23.3	15	3	10/11.03.87
2	23R	23.3	23R	23.3	15	15	16.06.87
3	28R	28.3	23R	23.3	4	4	7.10.87
4	28R	28.3	23R	23.3	4	4	5.11.87
5	23CW	23.3	23R	23.3	6	6	8/9.12.87
6	23CW	23.3	13CW	13.0	11	11	16/17.3.88
7	16CW	16.7	13CW	13.0	3	3	23/24.3.88
8	16CW	16.7	13CW	13.0	9	9	27/28.3.88
9	16CW	16.7	13CW	13.0	1	1	29.3.88
10	13CC	13.0	13CW	13.0	15	15	4–6.4.88
11	28R	28.3	23R	23.3	25	25	15–25.4.88
13	28R	28.3	23R	23.3	15	15	6/7.5.88

* As defined in Figure 2

** Not yet subject to any rejection (due to errors, unstationarity, . . .).

wind direction, as outlined in detail in Rotach (1993b). The values d_i for these wind direction sectors range from 9 to 16 m and thus correspond to d/h between 0.5 and 0.87, where h denotes the local building height (18.3 m). An average (over all wind direction sectors) $\langle d \rangle = 13.6$ m was computed, where the angular brackets denote a spatial average (see Section 3).

3. Concepts

The total turbulent transport of horizontal momentum in the vertical direction in the inertial sublayer is given by

$$\tau = \bar{\rho}(\overline{u'w'}^2 + \overline{v'w'}^2)^{1/2} . \tag{3}$$

This quantity is referred to as Reynolds Stress in the following. The friction velocity u_* is then

$$u_* = \left(\frac{\tau}{\bar{\rho}}\right)^{1/2} . \tag{4}$$

Under ideal conditions and with the x-axis of the coordinate system in the direction of the mean wind, the second term on the right hand side of (3), $\overline{v'w'}$, vanishes (Busch, 1973). However, the measurements of the fluctuating wind components at the present site show that even if the coordinate system is aligned with the mean wind direction for each run, the vertical flux of lateral momentum

($\sim \overline{v'w'}$) does not vanish completely for all runs. This indicates that the direction of the action of friction forces is not exactly aligned with the mean wind direction (if no horizontal averages are considered). As a consequence, the more general definition of Reynolds stress (from (3)) has been adopted for the calculation of the friction velocity. However, the results presented in the following sections are not sensitive to this definition of u_*.

3.1. Horizontal averages

As the flow within the UCL and RS is essentially three-dimensional, measurements or model predictions for a single point in the horizontal plane cannot lead to a general description of the flow. It is therefore appropriate to consider horizontal averages (Raupach and Shaw, 1982). Formally, an averaging operator can be defined (Raupach and Shaw, 1982) as

$$\langle \Omega \rangle = \frac{1}{A} \int_R \int \Omega(x, y)\, \mathrm{d}x\, \mathrm{d}y\,, \tag{5}$$

where Ω denotes a scalar field defined in the air but not at the points occupied by the roughness elements, and A is the area of a region R of the xy-plane. The angle brackets denote the horizontal average. In analogy to the decomposition of a time-dependent scalar flow variable into its mean and turbulent parts, we can write

$$\Omega(x, y, t) = \langle \Omega \rangle + (\Omega)''(x, y, t), \tag{6}$$

where the double prime indicates a departure from the horizontal average. Details on the properties of this averaging operator may be found in Raupach and Shaw (1982). In particular, they point out the importance of the sequence of temporal and spatial averaging. When the time averaging is applied first, an extra contribution to the Reynolds stress, the so-called dispersive covariance $\langle \bar{u}''\bar{w}'' \rangle$ is introduced. It arises from the spatial correlation of quantities averaged in time but varying with position. The total spatially averaged covariance then is

$$\langle u''w'' \rangle = \langle \bar{u}''\bar{w}'' \rangle + \langle \overline{u'w'} \rangle\,. \tag{7}$$

The dispersive covariance was estimated to be at least an order of magnitude smaller than $\langle \overline{u'w'} \rangle$ at the present site (Rotach, 1991). It is therefore neglected as suggested for many other flows (Mulhearn, 1978; Raupach *et al.*, 1986).

In contrast to wind tunnel experiments, where it is easily possible to obtain measurements at a sufficiently large number of horizontal positions in order to calculate horizontal averages according to Equation (5), this requirement is very difficult to meet in a field study. On the other hand, it can be argued that for different wind directions, a fixed instrument on a boom represents a variety of horizontal positions relative to the respective upwind (and downwind) geometry if there is no predominant wind direction. Thus, averaging over all runs with

different wind directions can be interpreted as an estimate of a horizontal average. However, a single measurement at one fixed location (e.g., above the roof) cannot provide information about the flow in another location (e.g., above a street canyon). When this first-order approximation for horizontal averages is used in the case of an urban RS or CL, it is therefore advisable to obtain measurements at more than one position in the horizontal plane to take different entities of urban morphology such as buildings or street canyons into account. At the present site, two positions in the horizontal plane were available immediately above the roof level (23.3 m) and within the canyon (13 m, see Figure 2). At these two levels, horizontal averages are estimated by averaging over both positions and all wind directions. At positions 28R and 16CW (Figure 2) averages are computed over all available runs (i.e., wind directions). Note that at the lowest position, i.e., at 13 m above street level, the measurements were taken below the zero plane displacement for certain wind direction sectors. If therefore RS characteristics are considered in the following, only those runs with $z - d_i \geq 0$ m are included into the analysis.

3.2. The scaling velocity

In order to compare observations at different heights, a scaling or reference velocity is defined that can be computed for all runs irrespective of the configuration (i.e, the combination of heights, cf. Table I) of the turbulence measurements:

$$u_{*r} = \frac{\mathrm{d}\bar{u}}{\mathrm{d}z'} \frac{kz'}{\Phi_m(z'/L)}, \tag{8}$$

where $z' = z - d$, and the stability (z'/L) is calculated from the gradient Richardson number (Businger *et al.*, 1971). The subscript 'r' refers to 'reference'. The function Φ_m is the semi-empirical function for the dimensionless wind shear. The formulation of Businger *et al.* (1971) modified after Högström (1988) has been used. The gradient of the mean wind speed is computed by fitting a second-order polynomial in $\ln(z')$ to the data and taking the derivative with respect to z'. Equation (8) is evaluated at the uppermost level of profile measurements (position 38R, Figure 2) thus assuming that

- this level is least disturbed by individual roughness elements
- horizontal inhomogeneity plays a minor role at this height (u_{*r} being independent of wind direction)
- inertial sublayer scaling is valid at this level of evaluation.

While the first assumption is obvious, it has been shown that horizontal inhomogeneity for roughness effects can be neglected already at lower heights, namely at position 28R (see II). The third assumption cannot be proved from the present data. However, as local scaling holds even closer to the roof level than position 38R (see II), Equation (8) assures that u_{*r} is at least related to Reynolds stress

at the level of evaluation. It is clear that the calculation of u_{*r} from the data at the end of a measured profile might be dangerous. However, the height variation of u_{*r} in the vicinity of position 38R is reasonably small (on the order of 0.01 s^{-1} or 2% per m, typically) thus indicating that the profiles are well behaved. The sensitivity u_{*r} to measurement uncertainties may furthermore be assessed as follows: when (artificially) changing the measured wind speed before the calculation of u_{*r} at either position 28R or 38R by ±2% (which corresponds to the absolute accuracy of the anemometers as given by the manufacturer), the resulting changes in u_{*r} are less than ±8%. Even if the gradients of mean wind speed and of potential temperature are crudely approximated by the respective finite differences, u_{*r} is found to be relatively little affected (less than 15%). Taking into account the error of a friction velocity if it had been directly measured, it is therefore concluded that u_{*r} from Equation (8) is reasonably well defined when evaluated at position 38R.

The measure for stability, z'/L, that is required for the calculation of Φ_m in Equation (8) will also be used to stratify the data according to stability if necessary. Taking the concept of local scaling into account, it can be identified with inertial sublayer stability to an extent that corresponds to the relation between u_{*r} and the proper IS friction velocity. Being determined at the largest possible distance from the surface, it refers to the most characteristic stability measure extractable from the present data set.

3.3. Conditional sampling

A useful tool for investigating the nature and mechanisms of turbulent processes is the method of conditional sampling. Contributions to the total mean Reynolds stress originate from four different quadrants in the (u, w)-plane. Following Raupach (1981) they are defined as:

- outward interaction, $i = 1$, $u' \geq 0$, $w' \geq 0$
- ejections, $i = 2$, $u' \leq 0$, $w' \geq 0$
- inward interactions, $i = 3$, $u' \leq 0$, $w' \leq 0$
- sweeps, $i = 4$, $u' \geq 0$, $w' \leq 0$.

Quadrants one and three give positive contributions and quadrants two and four negative contributions to the turbulent flux of momentum. Additionally, a hyperbolic hole H is defined, excluding from the analysis a region of instantaneous values of $|u'w'|$ that are smaller than $H \cdot |\overline{u'w'}|$. Systematic variation of the hole size H allows the investigation of the contributions to the total Reynolds stress, whether they are large and sparse or small and frequent. If [ ] denotes a conditional average, we have

$$[u'w']_{i,H} = \lim_{T_a \to \infty} \frac{1}{T_a} \int_0^{T_a} u'(t)w'(t)I_{i,H}(u'(t), w'(t))\,\mathrm{d}t\,, \tag{9}$$

where T_a is the averaging time and I the indicator function defined as

$$I_{i,H}(u', w') = \begin{cases} 1 & \text{if } (u', w') \text{ is in quadrant } i \text{ and} \\ & |u'w'| \geq H|\overline{u'w'}| \\ 0 & \text{otherwise.} \end{cases} \tag{10}$$

The stress fraction for quadrant i, $S_{i,H}$, is then

$$S_{i,H} = \frac{[u'w']_{i,H}}{\overline{u'w'}} \tag{11}$$

and the time fraction, $\delta_{i,H}$, is the average of $I_{i,H}$ over the time period of interest

$$\delta_{i,H} = \overline{I_{i,H}(u', w')}\,. \tag{12}$$

Note that through (11) the sum $S_{i,o}$ for $i = 1, 4$ at hole size zero is unity. Different quantities can be defined from the stress fractions. The difference ΔS_H between sweeps and ejections

$$\Delta S_H = S_{4,H} - S_{2,H} \tag{13}$$

or their respective ratio

$$\gamma = \frac{S_{2,o}}{S_{4,0}}\,, \tag{14}$$

at hole size zero. Both ΔS_H and γ are measures of the relative importance of sweeps and ejections. The exuberance E (Shaw *et al.*, 1983) is defined as

$$E = \frac{S_{1,o} + S_{3,o}}{S_{2,o} + S_{4,0}}\,, \tag{15}$$

i.e., the ratio of upward ($u'w' \geq 0$) to downward ($u'w' \leq 0$) flux of momentum. The exuberance may also be interpreted as the ratio of uncorrelated ('random') to organized contributions to the total turbulent transport of momentum. Within the inertial sublayer over a smooth surface, the exuberance is commonly about -0.16 (Raupach, 1981).

4. Height Dependence of Reynolds Stress

4.1. Observations

A comparison of the Reynolds stress simultaneously measured at two heights

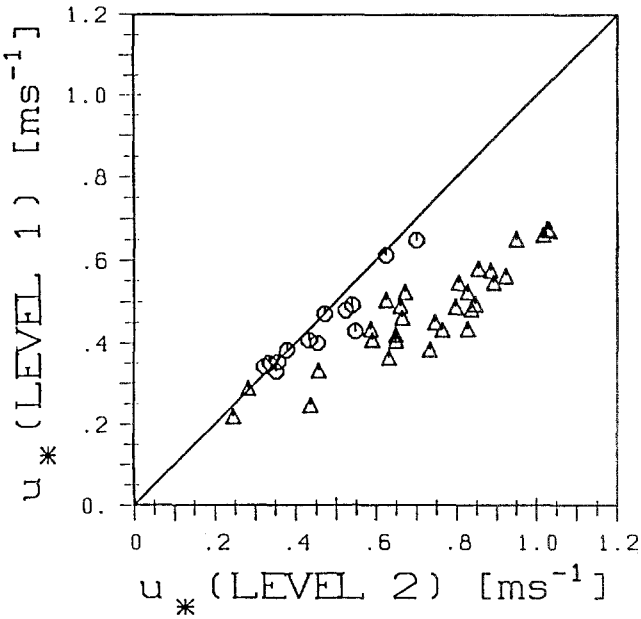

Fig. 3. Comparison of simultaneous u_* at different levels. Triangles: level 1 = position 23R and level 2 = position 28R. Diamonds: level 1 = position 23R, instrument #1; level 2 = position 23R, instrument #2. In the case of the diamonds, both instruments were mounted on the roof top tower, separated in the horizontal by about 2 m.

above the roof level is shown in Figure 3 (expressed as local friction velocity). 'Level 1' denotes position 23R (Figure 2), whereas 'level 2' refers either to position 28R (triangles) or to position 23R (diamonds). These latter runs (where both sonic anemometers were mounted on the roof top tower, approximately 2 m apart) have been included to make sure that the observed increase of Reynolds stress with height is not due to systematic instrument differences. Figure 3 shows that the Reynolds stress is systematically larger at the upper level, position 28R, compared to the lower level. The difference appears to be larger for large u_* and thus near-neutral stratification. However, the Obukhov length L also becomes essentially local if u_* is not constant with height, and in consequence the same applies to the measure of stability, z'/L.

Figure 4a shows the height dependence of Reynolds stress normalized with u_{*r} (see Section 3). There is a clear increase of Reynolds stress with height, with very small values at the lowest level. The scatter at the various positions of measurement is partly due to measurement uncertainties and partly due to horizontal inhomogeneity. It decreases with height as the latter decreases (see II). An indication of horizontal inhomogeneity is also given by the difference in the mean values at horizontally separated positions at the same level (positions 23R and 23CW, and 13CC and 13CW, respectively). At cross-canyon flow (Figure 4b) or flow parallel

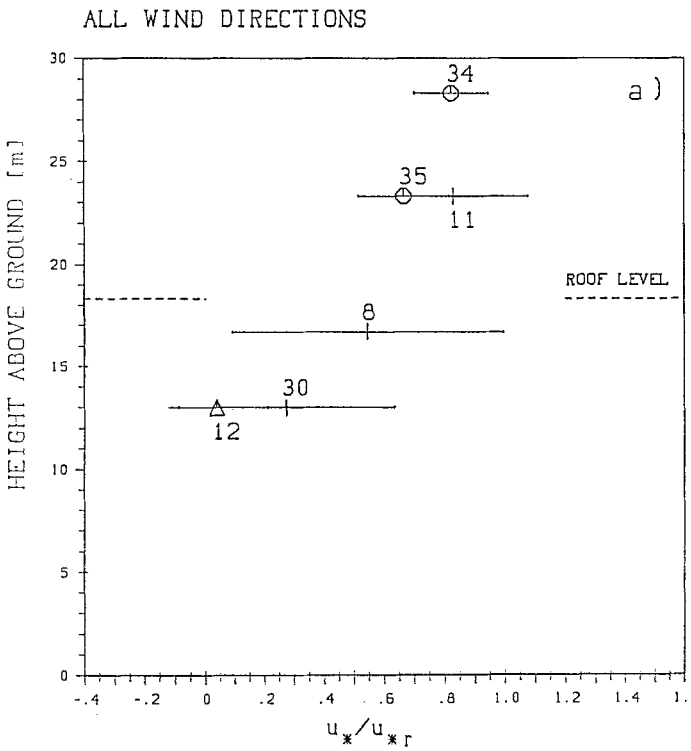

Fig. 4(a).

to the canyon, these differences tend to be more pronounced, while the run-to-run variability is clearly reduced. However, the requirements for horizontal averages as outlined in Section 3 cannot be met any longer due to the limited number of data at each level and due to the much weaker variation in upwind/downwind geometry. Thus any results concerning a wind direction dependence would be rather tentative and will not be discussed here. The gradient of the horizontally averaged Reynold stress seems to decrease with height, indicating that a constant value might be approached as observed in wind tunnel studies over rough surfaces (e.g., Raupach *et al.*, 1980).

Figures 5a–c show the scaled profiles of local u_* in three categories of stability. Again, the run-to-run variability is reduced at the various levels compared to Figure 4a. This indicates that stability affects the vertical profile of Reynolds stress and any model for this height dependence has to take this into account. While the near-neutral profile shows a less pronounced gradient and, in particular, non-negligible vertical transport of momentum within the canyon (position 13CW), the moderately unstable profile corresponds roughly to the overall mean (Figure 4a) and the strongly unstable profile is shifted towards smaller values.

As far as the author knows, there is no published study on the height dependence

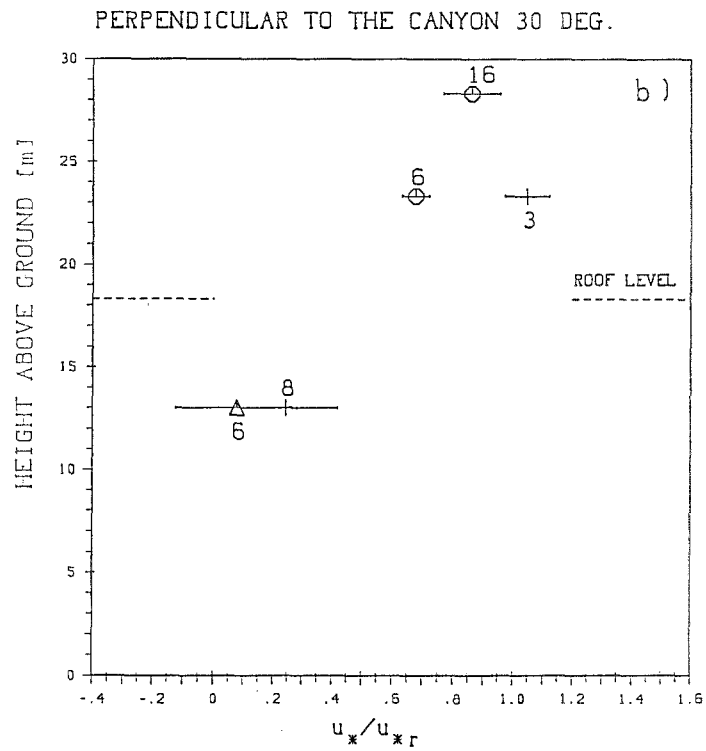

Fig. 4(b).

Fig. 4. Scaled profile of $u_*(z)$ for (a) all wind directions and (b) for approaching flow (above roof) within a sector of $\pm 30°$ from the northeast (orthogonal to the canyon). Error bars refer to run-to-run variability (standard deviation) and the numbers next to each symbol indicate the number of observations available to calculate average values (and variances). Diamonds: positions 23R and 28R; plus signs: positions 13CW, 16CW and 23CW; triangles: position 13CC.

of Reynolds stress in a comparable environment. However, in many wind tunnel experiments, where flow over rough surfaces was studied, a similar increase of Reynolds stress with height was observed (Antonia and Luxton, 1971; Mulhearn and Finnigan, 1978; Raupach *et al.*, 1980) but usually attributed to measurement difficulties close to the surface. Nevertheless, Mulhearn and Finnigan (1978) mention that it seems to be characteristic of a RS that Reynolds stress increases with height. On the other hand, Raupach *et al.* (1986) report an essentially constant Reynolds stress with height within the roughness sublayer over an artificial rough surface.

In the present case it can be excluded that the observed profiles of Reynolds stress are attributed to measurement errors. It can be ruled out that the two sonic anemometers differ systematically (Figure 3) or that the measurements at the lower levels are biased. Furthermore, a simple consideration shows that the observed

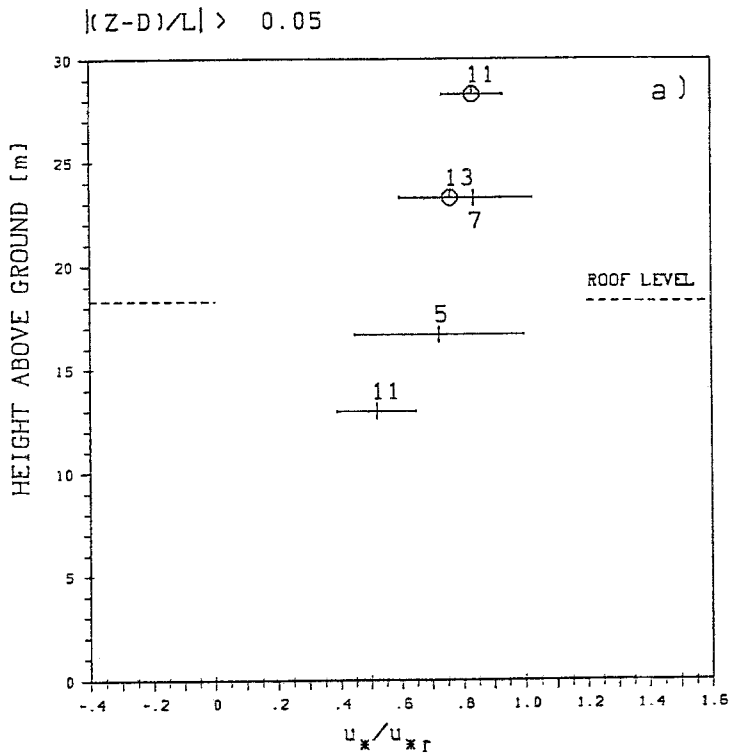

Fig. 5(a).

behaviour is consistent with the generally accepted picture of flow close to a surface: within the very first millimeters or centimeters above a smooth surface, the flow is laminar due to the small Reynolds number, and turbulent fluxes must vanish at the top of this layer. It seems therefore to be a helpful picture to consider the RS as the layer within which Reynolds stress increases from zero to the IS value. While this is a very thin layer (compared to the height of the IS) in the case of a smooth surface, it has a considerable vertical extension over a rough, e.g., urban surface. However, as Reynolds stress vanishes at a height close to the displacement height in the spatial average, the given analogy is only useful in a spatially averaged sense (with an appropriate horizontal averaging scale that will also considerably differ for smooth and rough surfaces). It is worth noting that the picture given above implies that the horizontal average of streamwise changes of pressure fluctuations, i.e., $\langle \partial p''/\partial x \rangle$, increases when approaching the 'surface' if viscous drag can be neglected (see Equation (18) in Section 5). This is consistent with observations of the pressure distribution around isolated obstacles such as an isolated fence (Jacobs, 1984).

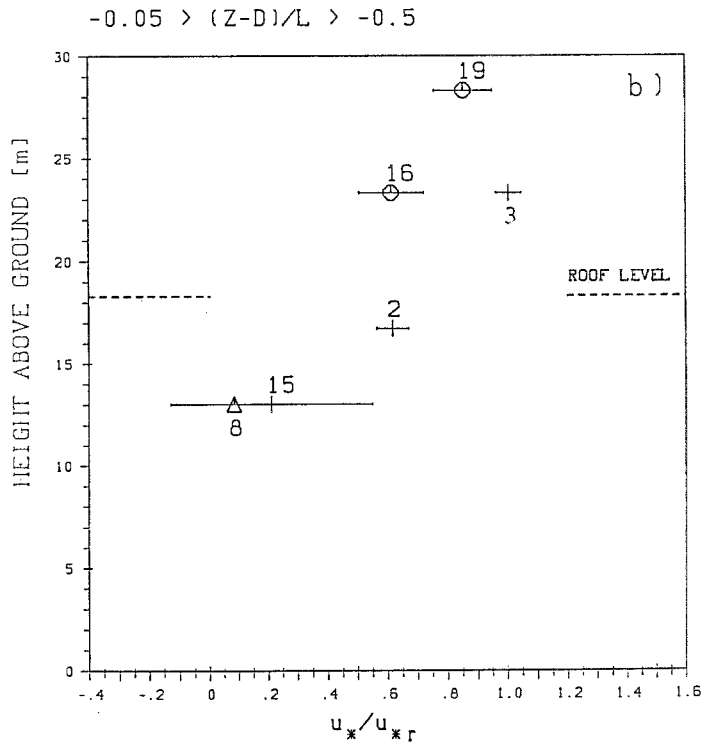

Fig. 5(b).

4.2. Parametric model

Assuming that an average of the scaled Reynolds stress over all wind directions and (where available) horizontal positions provides a reasonable measure for the horizontally averaged stress field (Section 3), the following statistical model for the height dependence of u_* can be formulated:

$$\frac{\langle u_*(z)\rangle}{u_{*r}} = C_1(1 - \exp\{-C_2 z'\})^{1/3} . \tag{16}$$

Here, C_1 and C_2 are numerical coefficients and the exponent 1/3 has been introduced without physical reasoning for better performance. The model has been designed such that Reynold stress vanishes at the zero plane displacement height in the horizontal average, thus referring to $z' = 0$ as the level of mean momentum absorption (Thom, 1971). Furthermore, Equation (16) ensures that at large z' a constant value is approached as can be expected from wind tunnel experiments (Antonia and Luxton, 1971; Raupach *et al.*, 1980) and seems also to be supported by the present data (Figure 4). For the parameter fit, the data of Figure 4a have been grouped into intervals of 2 m in z', for each of which an average $\langle u_*\rangle/u_{*r}$

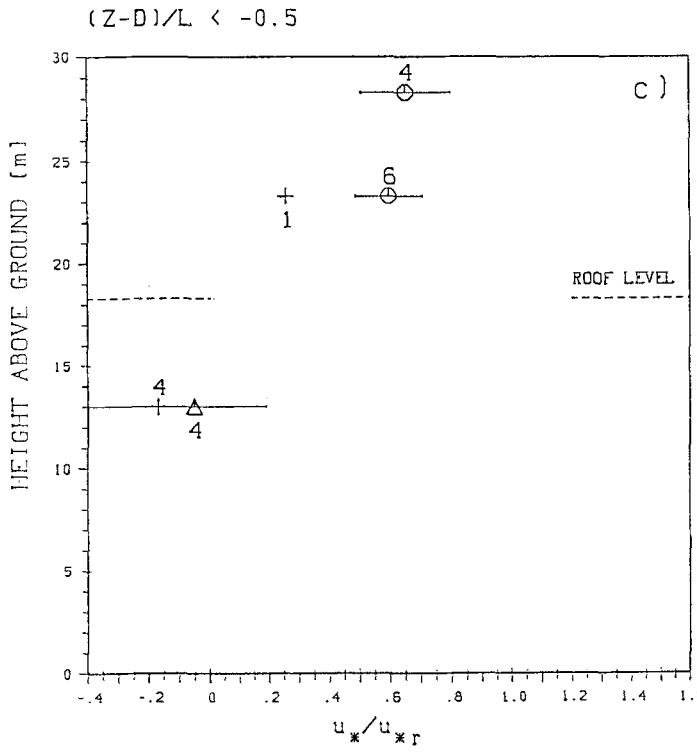

Fig. 5(c).

Fig. 5. As Figure 4, but for (a) near neutral ($|z'/L| \leq 0.05$), (b) weakly unstable and (c) strongly unstable runs. The stability is calculated as outlined in Section 3.2.

and z' was computed. The lowest interval was extended to slightly negative values of z' (but still $z' \geq -0.5$ m, i.e., the resolution of the zero plane displacement heights d_i) in order to avoid an average computed from too small an ensemble (with all three data points originating from the same wind direction sector). The parameter fit yields $C_1 = 1.19$ and $C_2 = 0.025$ with an rms difference between model and measurements of about 0.03 (Figure 6). For comparison, a linear model has also been evaluated which shows, however, a much larger rms difference (0.07) to the data besides not having physically reasonable asymptotic behaviour for large z' and $z' = 0$.

With the obtained parameters for the present site, $\langle u_* \rangle$ reaches a value of $1.19 u_{*r}$ at large z'. Thus it seems that the present reference friction velocity, u_{*r}, is still some 20% smaller than the 'true' IS friction velocity u_*^{IS} and all the measurements were taken entirely within the RS. An evaluation of the height of the roughness sublayer, z_* is therefore not possible from the present data set.

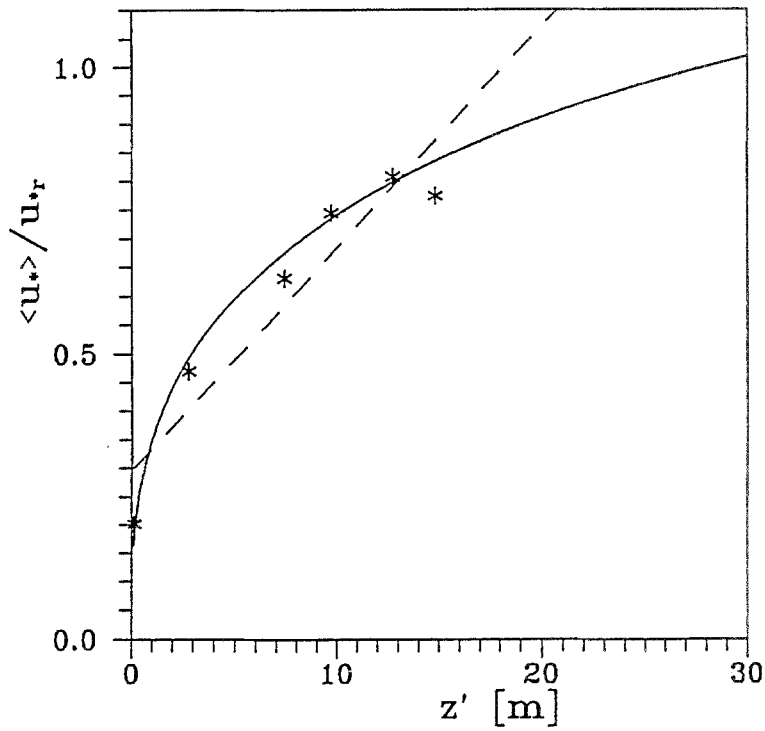

Fig. 6. Scaled profile of local friction velocity. Shown are the measurements averaged over intervals of 2 m in z'. The parametric model, Equation (16), is shown as the full line and a linear best fit is given by the dashed line.

5. Resulting Profile of Mean Wind Speed

Considering a thin layer of height δz within the roughness sublayer, the turbulent transport supplies this layer with momentum from above. Due to the decrease of Reynolds stress near the surface, the turbulent transport through the bottom of this layer is diminished resulting in a profile of mean wind with a smaller gradient than a semi-logarithmic profile. Close to the surface, the wind speed must therefore be larger than predicted by Equation (8). This qualitative behaviour is in agreement with wind tunnel observations of Raupach *et al.* (1980).

Assuming that local scaling holds for the non-dimensional gradient of mean wind speed, i.e.

$$\frac{\mathrm{d}\bar{u}}{\mathrm{d}z'}\frac{kz'}{u_*(z')} = \Phi_m(z'/L(z'))\,, \tag{17}$$

where $u_*(z')$ refers to Equation (16), the profile of mean wind speed can be calculated. This was done for all runs by numerically integrating Equation (17)

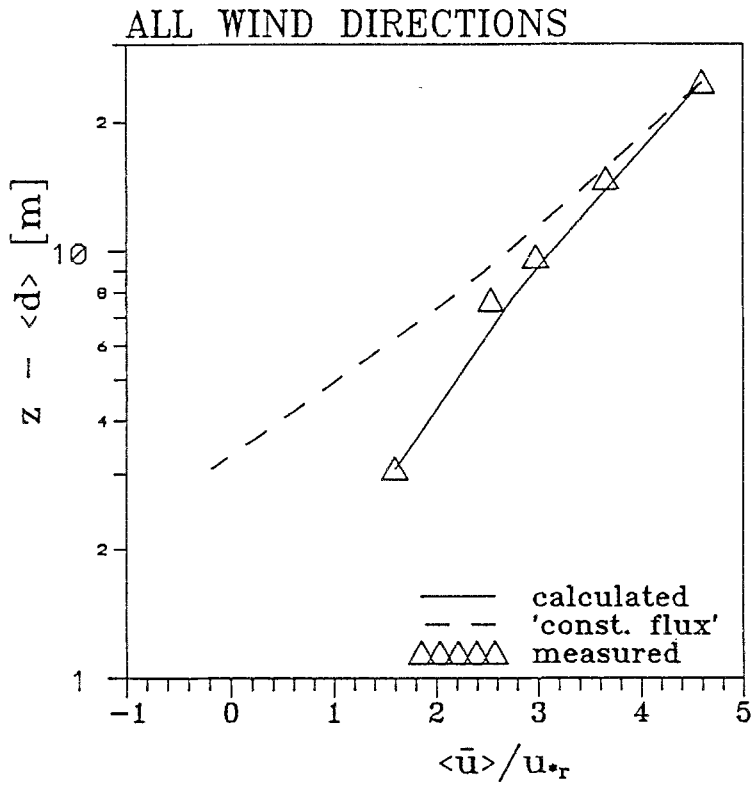

Fig. 7. Average profiles of scaled wind speed. 'Calculated' refers to Equation (17). 'Constant flux' was calculated with $u_*(z) = \text{const.} = u_{*r}$ and $\theta_*(z) = \text{const.} = \theta_{*r}$. The latter quantity is defined in analogy to u_{*r}.

downward from the uppermost level (position 38R). The turbulent flux of sensible heat (for the calculation of the local Obukhov length $L(z')$) was parameterized based on data presented in Rotach (1991). Finally, all the profiles are scaled with u_{*r} and averaged. In Figure 7, this average 'calculated' profile is compared to the measured profile, which was averaged in the same manner. Note that the lowest two profile-levels within the canyon are not included since they are located below the mean zero plane displacement height and thus, Equation (16) may not be applied. It can be seen that the correspondence between calculated and measured average profiles is excellent. For comparison, a 'constant flux' profile was calculated in the same manner but with assumed constant turbulent fluxes of momentum (corresponding to u_{*r}) and sensible heat. Figure 7 shows that the observed profile of turbulent transport of momentum explains the measured profile of mean wind speed. This result is, in fact, another way of stating that local scaling is a useful approach for momentum in the roughness sublayer (see II).

The above result concerning the profile of mean wind speed raises the question:

how is the observed gradient of Reynolds stress balanced in the momentum conservation equation? The horizontally averaged streamwise Navier–Stokes equation for stationary conditions and neutral flow (no buoyancy forces) within and above a canopy can be written as (Raupach and Shaw, 1982)

$$\langle \bar{u} \rangle \frac{\partial \langle \bar{u} \rangle}{\partial x} + \langle \bar{w} \rangle \frac{\partial \langle \bar{u} \rangle}{\partial z} + \frac{\partial}{\partial z} \langle \overline{u'w'} \rangle + \frac{\partial}{\partial x} \langle \overline{u'u'} \rangle =$$

$$= -\frac{1}{\bar{\rho}} \frac{\partial \langle \bar{p} \rangle}{\partial x} - \frac{1}{\bar{\rho}} \left\langle \frac{\partial p''}{\partial x} \right\rangle + \nu \langle \nabla^2 u'' \rangle \,, \tag{18}$$

where the last two terms on the rhs represent the forces per unit mass of air exerted by form and viscous drag, respectively. Within the canopy (i.e., below roof level), where the largest gradient of Reynolds stress occurs, it is most likely balanced by the spatial distribution of drag forces (the second term on the rhs of Equation (18)) (assuming that viscous forces can be neglected). Higher up, in the roughness sublayer, where this contribution is zero, the gradient of Reynolds stress is still of the order $10^{-2}\,\mathrm{m\,s^{-2}}$ (Equation (16)) and must be balanced either by advection (the first two terms on the lhs of Equation (18)) or by a mean horizontal gradient of turbulence kinetic energy or pressure on a scale larger than the horizontal averaging scale. Mesoscale features like the urban heat island or a distinct increase in surface roughness have to be taken into account to assess the relative importance of the various terms in Equation (18). Considering highly idealized model results for a step change in surface roughness (Claussen, 1987) and a heat island (Lüthi *et al.*, 1989), it is found that the advective terms and the horizontal gradient of turbulent kinetic energy are all at least an order of magnitude too small (apart from very close to the roughness change) to balance the measured gradient in Reynolds stress. The vertical advection term has furthermore the wrong sign. On the other hand, both these processes which are typical for urban scale flow modification, lead to a negative mean horizontal pressure gradient (over the heated or rougher surface, respectively) that is of the required order of magnitude. Thus an explanation for the Reynolds stress gradient may be the mesoscale pressure distribution of an urban area due to thermal and/or roughness effects.

6. Conditional Sampling for Reynolds Stress

The Reynolds stress field within and above the street canyon was examined using the technique of conditional sampling (see Section 3) in order to illustrate the effect of forces exerted on the flow by form drag at different heights. Figure 8 shows the vertical distribution of the averaged stress fractions at hole size zero, $S_{i,o}$. At the uppermost level, outward and inward interactions are small with almost the same numerical value while sweeps ($i = 4$) slightly dominate ejections ($i = 2$) (see Table II). These stress fractions are similar to those observed in an inertial sublayer by Raupach (1981). At the 23.3 m level, the dominance of sweeps

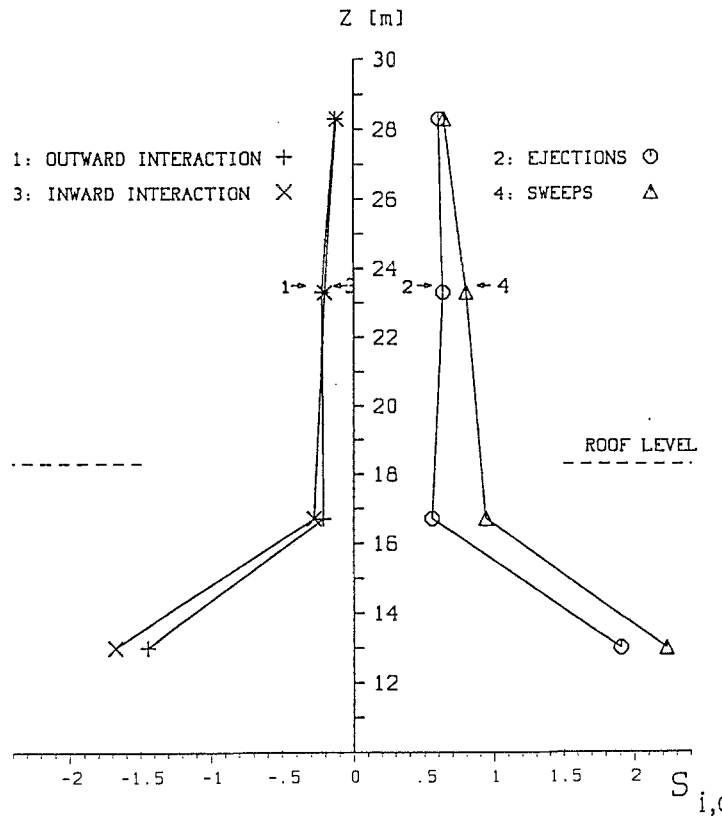

Fig. 8. Averaged vertical profiles of the four contributions to Reynolds stress $S_{i,o}$, $i = 1, 2, 3, 4$. At the second highest level ($z = 23.3$ m) $S_{i,o}$ is computed as an average of measurements at positions 23R and 23CW, respectively.

TABLE II

Parameters related to quadrant analysis. For definitions see Section 3

Position	z (m)	z/h	$S_{2,o}/S_{4,o}$	ΔS_o	E^*
28R	28.3	1.55	0.921	0.051	−0.190
23R	23.3	1.27	0.887	0.107	−0.415
23CW	23.3	1.27	0.655	0.273	−0.237
16CW	16.7	0.91	0.592	0.383	−0.331
13CW	13	0.71	0.856	0.321	−0.758

* Exuberance as defined in Equation (15)

is much more pronounced, mainly due to the 'above canyon' runs (position 23CW), whereas the ratio between $S_{2,0}$ and $S_{4,0}$ above the roof remains unchanged compared to 28.3 m. Below roof level the contribution of sweeps further increases and thus ΔS_0, the difference between $S_{4,0}$ and $S_{2,0}$, becomes larger ($S_{2,0}/S_{4,0}$ smaller).

The large contributions of all stress fractions at the lowest level arise from averaging over a number of runs with small, sometimes positive momentum transport. At this height, the total turbulent flux of momentum is often found to be small due to near cancellation of large absolute contributions of the individual sectors with opposite signs. Note that for the averaging as shown in Figure 8, those runs with total Reynolds stress smaller than $0.05\,m^2\,s^{-2}$ were excluded to avoid the results being dominated by single runs (this essentially affects only the contributions at the lowest levels and in particular in the mid-canyon position 13CC. For this position none of the runs surpassed the threshold given above).

A comparison of the exuberances (i.e., the ratio of upward to downward transport of momentum, Equation (15)) at the two levels above the roof (Table II) shows the increasing importance of inward and outward interactions at 23.3 m compared to the upper level. These arise from the disturbance of the more or less organized shear flow at a presumably small length scale. Figure 9 illustrates this in an example. While the fluctuations of the longitudinal component are often similar at both heights, the low-frequency variations of w' are broken up at the lower level into fluctuations of higher frequency that are less correlated to the u'-component. This leads to the larger contributions of interactions at the expense of sweeps and ejections close to the surface. Furthermore, from Figure 10 it is evident that for the lower level above the roof, the larger contribution of Sectors 1 and 3 is due to small-scale turbulent motion. For example, the contribution of inward interactions, $S_{3,0}$ at position 23R is approximately -0.34 while at position 28R, $S_{3,0} \sim -0.11$. For hole size 5, on the other hand, the contribution of inward interactions is already smaller than -0.05 at both heights.

The contributions of the four quadrants at varying hole sizes and for the different heights (Figure 10) indicate that sweeps are associated with processes of much larger scale than ejections. Particularly at positions 23CW and 16CW, closely above and below roof level, respectively, significant contributions to momentum transport due to sweeps occur at hole sizes up to 30. To a somewhat lesser extent, this is also observed at position 23R but not at the uppermost level. This behaviour indicates that momentum is transported into the street canyon by sporadically penetrating eddies from above. From Figure 10, a tendency for increasing, partly offsetting contributions from the four quadrants can be observed with decreasing height at both positions in the horizontal plane (i.e., 'above roof' and 'above and within the canyon'). This is a further indication for the 'disorganisation' of the flow or, in other words, the reduction of correlation between the u'- and w'-fluctuations when approaching the surface due to wake pressure effects. Figure 11 gives a comparison between the summed stress and time fractions (Equation (12)) as a function of hole size and at different heights as a measure for intermittency. The most intermittent turbulence is observed at the 16.7 m level. Here, about 70% of the total momentum transfer at hole size 5 occurs during less than 10% of the time and the ratio between total time fractions and total stress fractions is only 0.129 (cf. Table III). At the other extreme, the level near the zero-plane

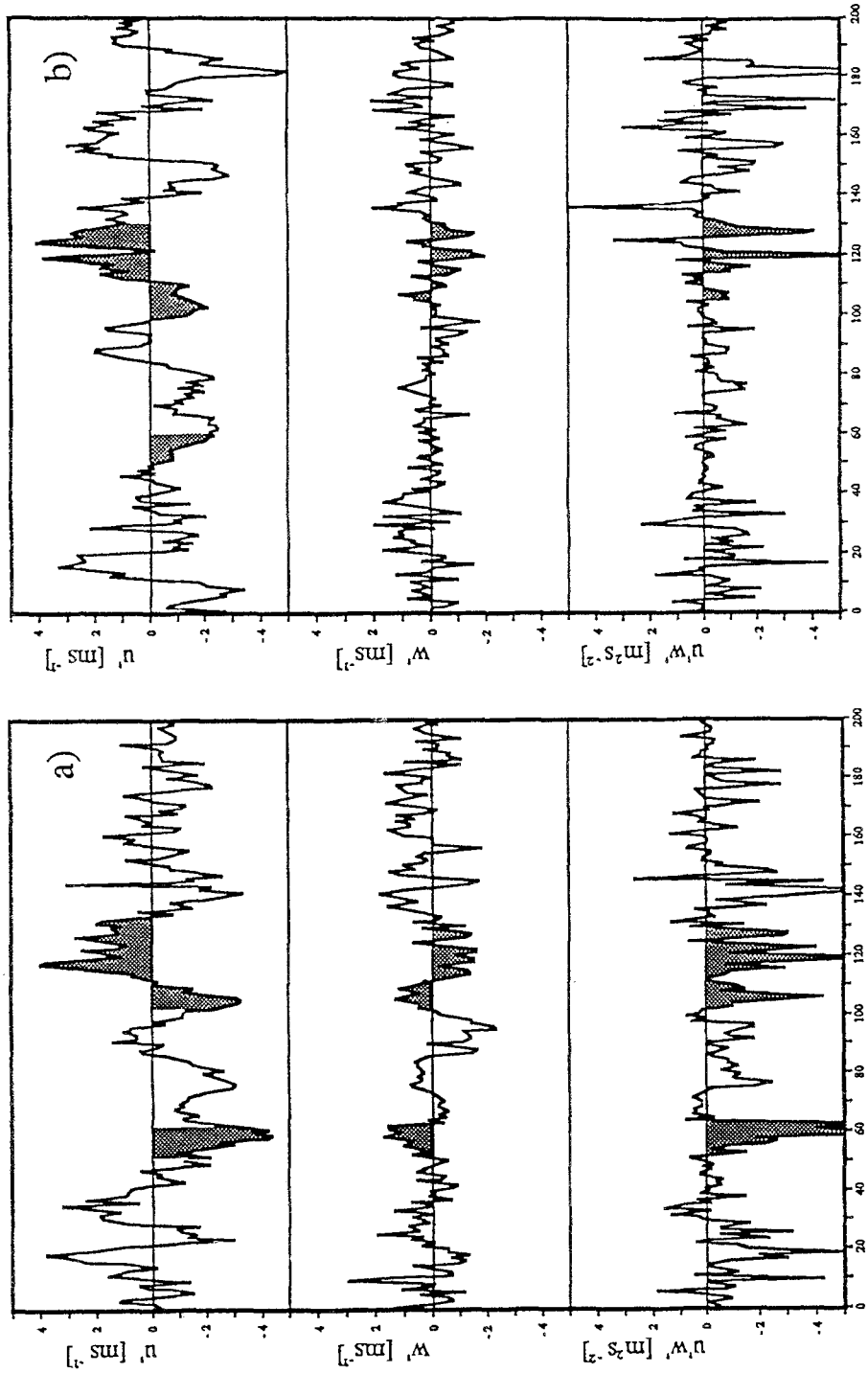

Fig. 9 Time series of u', w' and $u'w'$ for an arbitrarily chosen interval of 200 s. (a) position 28R and (b) position 23R. Shaded areas emphasize time intervals during which sweeps and ejections observed at the upper level appear as outward or inward interactions 5 m closer to the surface.

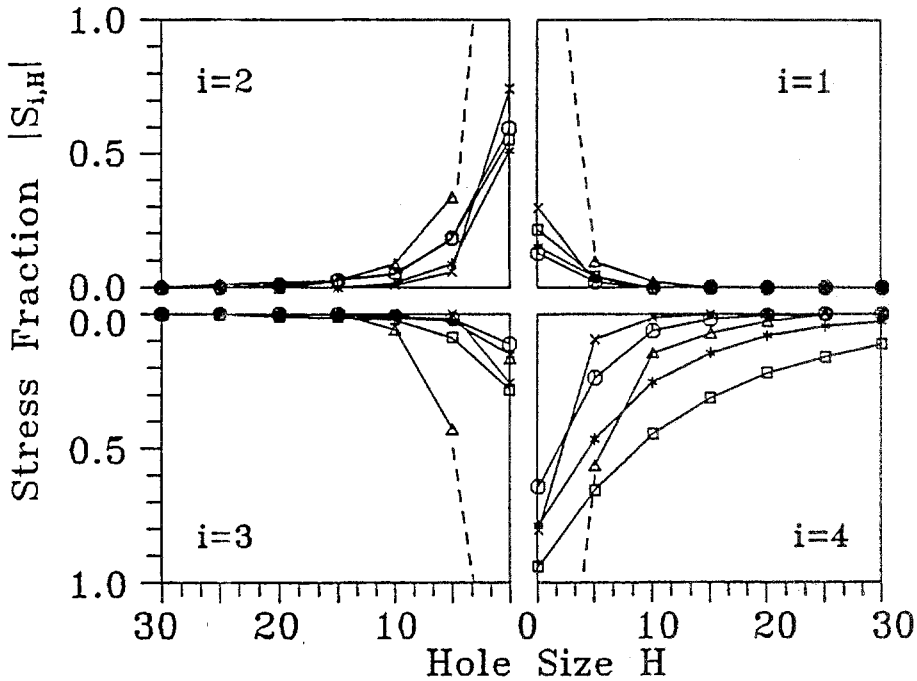

Fig. 10. Magnitude of the stress fractions, $|S_{i,H}|$, ($i = 1, 2, 3, 4$) for varying hole sizes H. The symbols refer to the measurement positions. Diamonds: 28R; crosses: 23R; stars: 23CW; squares: 16CW, triangles: 13CW. Large numbers in the corner of each box denote the quadrant number i.

displacement height within the canyon (position 13CW), large fractions of total stress occur up to hole size 30 during an almost comparable fraction of time (note, that total stress is very close to zero on average at this height). There are no significant differences in intermittency between the three positions above roof level (Table III). From the aforementioned observations, the general features of the transport of momentum close to an urban surface may be summarized as follows:

- The organized shear flow, characterized by the IS type of distribution of stress contributions at a mid roughness-sublayer position, is distorted when approaching the surface due to wake pressure effects, resulting in a less correlated flow structure.
- As a result, the exuberance decreases from -0.2 at the mid RS position to -0.8 at the 'surface' (i.e. the zero plane displacement).
- At a given horizontal position, the stress contributions of any sector increase when approaching the surface. This again illustrates the uncorrelated ('random') nature of turbulence close to the ground.

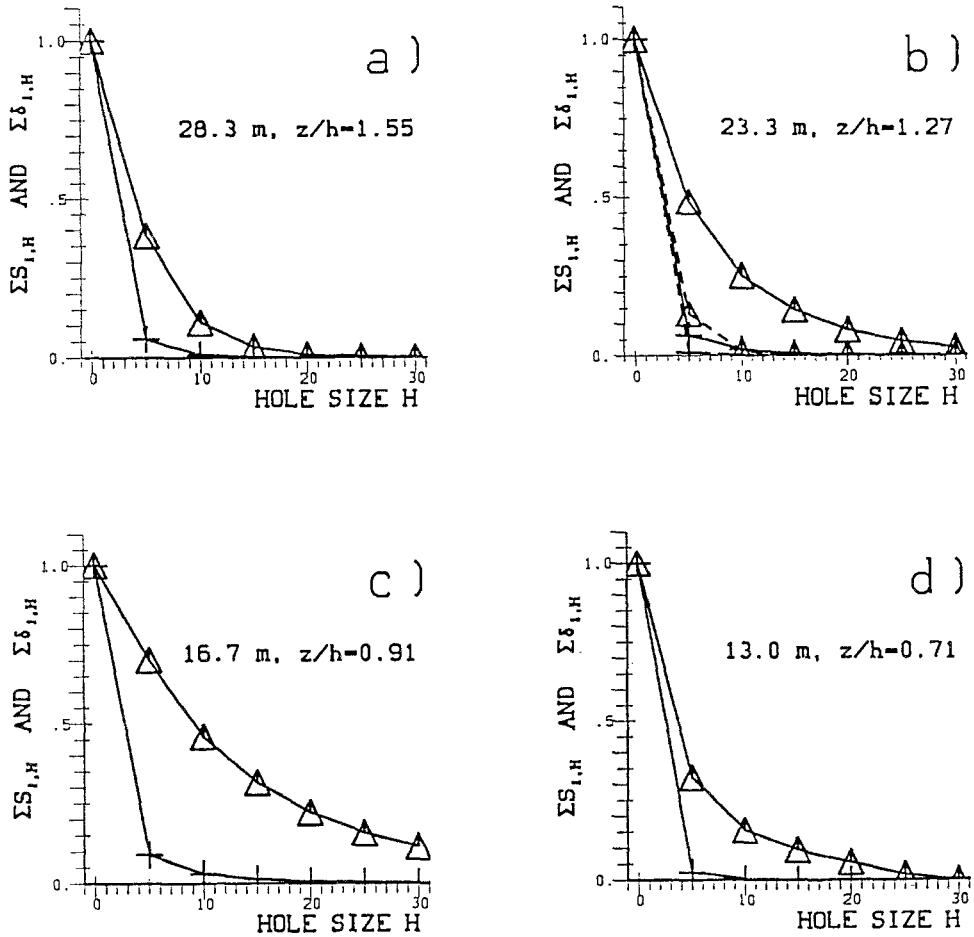

Fig. 11. Comparison of the summed stress fractions $\Sigma S_{i,H}$ ($i = 1$ to 4, triangles) and the summed time fractions $\Sigma \delta_{i,H}$ ($i = 1$ to 4, plus signs) for different hole sizes H. (a) position 28R, (b) position 23R (solid lines) and position 23CW (dashed lines, above canyon), (c) position 16CW and (d) position 13CW.

TABLE III

The ratio of summed time fractions to summed stress fractions $\Sigma \delta_{i,H}/\Sigma S_{i,H}$ ($i = 1$ to 4) at hole sizes 5 and 10

Height z (m)	Hole size 5	Hole size 10
28.3	0.166	0.081
23.3 (23R)	0.199	0.111
23.3 (23CW)	0.171	0.092
16.7	0.129	0.065
13	0.633	0.571

TABLE IV

Characterization of turbulent transport of momentum at various non-dimensional heights in an urban roughness sublayer

z/h	Position	Characteristics
1.55	28R	About 30% of total stress contributions occur at hole sizes smaller than 5. Sweeps slightly dominate ejections. Small interactions. Distribution of contributions similar to IS behaviour.
1.27	23R	Enhanced contributions from the interactions (as compared to $z/h = 1.55$). Tendency to smaller scale transport of momentum (40% of total stress contribution at hole size smaller than 5). Sweeps slightly dominate over ejections. All $S_{i,o}$ larger than at $z/h = 1.55$.
1.27	23CW	Sweeps clearly dominate ejections at all hole sizes, while the interactions are much smaller than at the same height above the roof. No enhanced intermittency compared to positions 23R and 28R.
0.91	16CW	Transport of momentum occurs at large hole sizes (more than 70% of total stress at hole sizes larger than 5) and strongly intermittent. Downward transport is partially offset by upward transport (interactions). Sweeps clearly dominate.
0.71	13CW	Almost no net transport of momentum with large contributions $S_{i,o}$ (larger than 1) from all sectors. Large stress fractions at hole sizes up to 30 also with considerable time fractions at this hole size.

- Sweeps contribute much more to momentum exchange between the street canyon and the urban RS than ejections. Their dominance decreases with height.
- Transport of momentum is most intermittent immediately below the roof level while at the mid-canyon position, the (very small) net transport of momentum is highly continuous. Between the three positions above the roof level, no large variation in intermittency can be observed.

A characterization of the momentum transport at the various (non-dimensional) heights is given in Table IV.

The present results are in good agreement with measurements by Raupach (1981) for artificial rough and smooth surfaces in a wind tunnel study. The inertial sublayer is identified in these wind tunnel experiments as a layer with $S_{2,o} \simeq S_{4,o} \simeq 0.6$, both having significant contributions at $H \geq 10$, whereas $S_{1,o} \simeq S_{3,o} \simeq -0.1$ with vanishing contributions for $H \geq 5$. Within the roughness sublayer over the roughest surface, sweeps dominate the turbulent transport of momentum and have significant contributions to total stress up to $H \geq 20$, whereas ejections cease to contribute already at $H \geq 5$. The main differences to the present observations are:

- Raupach (1981) observes clear roughness sublayer behaviour at $z/h = 1.46$, whereas at a comparable height, $z/h = 1.55$, over the urban surface, the distribution of the four quadrants tends towards inertial sublayer behaviour.
- The rapid decrease of contributions from ejections as the hole size increases, is not so pronounced in the urban RS as observed in the wind tunnel. However,

Raupach points out that the ratio of sweeps to ejections (or the difference between them) is strongly dependent on the density of roughness elements.

- The behaviour of Raupach's 'within canopy' level ($z/h = 0.53$) compares to the present position 16CW ($z/h = 0.91$) rather than to position 13CW ($z/h = 0.71$). However, this is associated with considerably larger total downward transport of momentum at the mid-canopy height in the wind tunnel experiment than at the present position 13CW (see the results of Raupach *et al.*, 1980). It seems, that for '*d*-type' roughness (in the notation of Perry *et al.*, 1969) where recirculating vortices can be formed behind roughness elements (as can be anticipated for the present case), ejections do not dominate momentum transfer (Townsend, 1976), but rather momentum transfer is stopped at a certain level (identified to be the mean zero plane displacement in the present study).

This last point is also the main discrepancy when comparing the present results to a corn canopy flow (Shaw *et al.*, 1983). For this type of canopy, no decrease of the exuberance (to larger negative values) with decreasing height was observed but rather a relatively constant value of -0.2. It arose from approximately constant contributions (within the canopy) from the interactions while the contribution of sweeps increases with decreasing height (in the upper half of the canopy) and that of ejections decreases. Within and above a deciduous forest (Baldocchi and Meyers, 1988), the vertical structure of the stress field is also similar to the present results in some respects. At a level within the crown area, where the total momentum transfer is already small compared to above-canopy values, the contributions to total stress from the four quadrants become very large ($\geqslant 1.5$) and partially offset each other. Furthermore, the exuberance within a deciduous forest canopy ranges between -0.3 and -0.8 (associated with small total momentum transport) comparable to the values found for the UCL. Baldocchi and Meyers (1988) argue that large (negative) exuberance values may be associated with wake turbulence and secondary circulations. The present urban canopy, for which the importance of wake effects has been shown earlier and the presence of vortices can be assumed (at least in some cases with appropriate wind direction), strongly supports this hypothesis.

7. Summary and Conclusions

Measurements from a site in the centre of a major city shows that Reynolds stress increases with height within the urban roughness sublayer. Vertical turbulent transport of momentum is found to be negligible at a height close to the average zero plane displacement $\langle d \rangle$. It is shown that this height dependence of Reynolds stress does not result from measurement errors. The profile of Reynolds stress within the roughness sublayer reduces the gradient of mean wind speed with respect to the inertial sublayer prediction. However, it is shown that turbulent

transport is still the relevant process that counteracts the loss of momentum due to frictional forces close to the surface.

The above characteristics of Reynolds stress are valid if horizontal averages are considered. In the present study, horizontal averages have been approximated using measurements at fixed positions in the horizontal plane, but with different directions of the approaching wind. Thus each location represents a variety of upwind (and downwind) geometries. The average profile of Reynolds stress has been parameterised describing the local friction velocity, $u_*(z)$, in terms of the height above the zero plane displacement and a reference u_{*r}. Similar characteristics of Reynolds stress have been observed in roughness sublayers over artificial rough surfaces. Nevertheless, it remains to be shown to what extent the observed profile of Reynolds stress can be considered typical for an urban roughness sublayer. In particular, it will have to be examined in greater detail (and using data from various sites) in what way building geometry determines the shape of the Reynolds stress profile.

As the roughness elements are approached, the flow's 'organized' turbulence structure is broken up into small-scale disturbances, resulting in larger ('random') upward and smaller ('organized') downward contributions to total momentum transfer. The use of the conditional sampling technique shows that this behaviour is associated with a tendency for increasing, partly offsetting contributions from the four quadrants and for increasing negative values of the exuberance with decreasing height. Furthermore, sweeps are found to be far more important than ejections for the exchange between canyon air and the roughness sublayer above. The most intermittent turbulence is observed closely below roof level where considerable contributions to momentum transport occur at hole sizes up to 30. In general, the results from the quadrant analysis of momentum transport are in good agreement with those reported from artificial or vegetated rough surfaces.

The results presented here may have some important consequences on urban diffusion modelling. First it is noted that there exists an urban roughness sublayer with a vertical extension of a few times the building height. At the present site, this layer is characterized by the non-constant Reynolds stress and the requirement of local scaling (see II). The present observations indicate that the flow characteristics in the RS are altered with respect to surface-layer similarity predictions (which are commonly used in practice throughout the roughness sublayer). Both advection through the modified profile of mean wind speed and turbulent mixing are affected. However, the question to what extent the present results for momentum transport apply to turbulent transport of scalars (e.g., a pollutant) remains unanswered and further experimental and conceptual effort is needed.

Acknowledgements

I am very obliged to Drs. H. P. Schmid, S.-E. Gryning and M. Roth for valuable discussions and critical comments on the manuscript. Dr. M. R. Raupach provided

a very important comment on the first draft of the manuscript that is greatly appreciated. I am very grateful to Karl Schroff who was in charge of the measurements and who found a solution to almost any unsolvable problem. Many thanks are also due to Drs. A. Ohmura, H. C. Davies and T. R. Oke for their support during and at the end of this study, which is part of a doctoral thesis. Funding was provided by the Swiss National Science Foundation (Grants 2.580-0.84/2.220-0.86).

References

Antonia, R. A. and Luxton, R. E.: 1971, 'The Response of a Turbulent Boundary Layer to a Step Change in Surface Roughness, Part I: Smooth to Rough', *J. Fluid Mech.* **48**, 721–761.

Baldocchi, D. D. and Meyers, T. P.: 1988, 'Turbulence Structure in a Deciduous Forest', *Boundary-Layer Meteorol.* **43**, 345–364.

Bendat, J. S. and Piersol, A. G.: 1986, *Random Data; Analysis and Measurement Procedures*, John Wiley, New York, 407 pp.

Busch, N. E.: 1973, 'On the Mechanics of Atmospheric Turbulence', in D. A. Haugen (ed.), *Workshop on Micrometeorology*, Amer. Meteorol. Soc., Boston, Massachusetts, pp. 1–65.

Businger, J. A., Wyngaard, J. C., Izumi, Y., and Bradley, E. F.: 1971, 'Flux-Profile Relationships in the Atmospheric Surface Layer', *J. Atmos. Sci.* **28**, 181–189.

Claussen, M.: 1987, 'The Flow in a Turbulent Boundary Layer Upstream of a Change in Surface Roughness', *Boundary-Layer Meteorol.* **40**, 31–86.

Gross, G.: 1989, 'Numerical Simulation of the Nocturnal Flow Systems in the Freiburg Area for Different Topographies', *Beitr. Phys. Atmosph.* **62**, 57–72.

Gryning, S.-E. and Lyck, E.: 1984, 'Atmospheric Dispersion from Elevated Sources in an Urban Area: Comparison between Tracer Experiments and Model Calculations', *J. Clim. Appl. Meteorol.* **23**, 651–660.

Högström, U., Bergström, H. and Alexandersson, H.: 1982, 'Turbulence Characteristics in a Near-Neutrally Stratified Urban Atmosphere', *Boundary-Layer Meteorol.* **23**, 449–472.

Jacobs, A. F. G.: 'Static Pressure Around a Thin Barrier', *Arch. Met. Geoph. Biocl., Ser. B*, **35**, 127–135.

Lüthi, D. Schär, C., and Davies, H. C.: 1989, 'On the Atmospheric Response to Steady Mesoscale Low-Level Diabatic Heating', *Beitr. Phys. Atmosph.* **62**, 126–150.

Mulhearn, P. J.: 1978, 'Turbulent Flow over a Periodic Rough Surface', *Phys. Fluids.* **21**, 1113–1115.

Mulhearn, P. J. and Finnigan, J. J.: 1978, 'Turbulent Flow over a very Rough, Random Surface', *Boundary-Layer Meteorol.* **15**, 109–132.

Oke, T. R.: 1988, 'The Urban Energy Balance', *Prog. Phys. Geogr.* **12**, 471–508.

Perry, A. E. Schofield, W. H., and Joubert, P. N.: 1969, 'Rough Wall Turbulent Boundary Layers', *J. Fluid Mech.* **37**, 383–413.

Raupach, M. R.: 1981, 'Conditional Statistics of Reynolds Stress in Rough-Wall and Smooth-Wall Turbulent Boundary Layers', *J. Fluid Mech.* **108**, 363–382.

Raupach, M. R. and Shaw, R. H.: 1982, 'Averaging Procedures for Flow within Vegetation Canopies', *Boundary-Layer Meteorol.* **22**, 79–90.

Raupach, M. R., Thom, A. S., and Edwards, I.: 1980, 'A Wind-Tunnel Study of Turbulent Flow Close to Regularly Arranged Rough Surfaces', *Boundary-Layer Meteorol.* **18**, 373–397.

Raupach, M. R. Coppin, P. A., and Legg, B. J.: 1986, 'Experiments on Scalar Dispersion within a Model Plant Canopy. Part I: The Turbulence Structure', *Boundary-Layer Meteorol.* **35**, 21–52.

Rotach, M. W.: 1990, 'Turbulence in an Urban Transition Layer', *Proceedings 9th Symposium on Turbulence and Diffusion*, Roskilde, Denmark, pp. 289–292.

Rotach, M. W.: 1991, 'Turbulence Within and Above an Urban Canopy', ETH Diss. 9439, 240 pp. Published as *ZGS*, Heft 45, Verlag vdf, Zürich, 1991.

Rotach, M. W.: 1993a, 'Turbulence Close to a Rough Urban Surface Part II: Variances and Gradients', *Boundary-Layer Meteorol.*, accepted for publication.

Rotach, M. W.: 1993b, 'Determination of the Zero Plane Displacement in an Urban Environment', *Boundary-Layer Meteorol.*, submitted for publication.

Shaw, R. H., Tavangar, J., and Ward, D. P.: 1983, 'Structure of Reynolds Stress in a Canopy', *J. Clim. Appl. Meteorol.* **22**, 1922–1931.

Thom, A. S.: 1971, 'Momentum Absorption by Vegetation', *Quart. J. Roy. Meteorol. Soc.* **97**, 414–428.

Townsend, A. A.: 1976, *The Structure of Turbulent Shear Flow*, 2nd ed., Cambridge University Press, Cambridge, 429 pp.

Wyngaard, J. C.: 1973, 'On Surface Layer Turbulence', in D. A. Haugen (ed.), *Workshop on Micrometeorology*, Amer. Meteorol. Soc., Boston, pp. 101–150.